Vitamin D Deficiency Promotes Prostate Cancer Growth in Bone

Yu Zheng,[1,2] Hong Zhou,[1] Li Laine Ooi,[1] Afik D. Snir,[3] Colin R. Dunstan,[1,3] and Markus J. Seibel[1,4]*

[1]*Bone Research Program, ANZAC Research Institute, University of Sydney, Concord, Sydney, NSW, Australia*
[2]*Cancer Research Program, Garvan Institute of Medical Research, Darlinghurst, Sydney, NSW, Australia*
[3]*Biomedical Engineering, AMME, University of Sydney, Sydney, NSW, Australia*
[4]*Department of Endocrinology and Metabolism, Concord Hospital, University of Sydney, Concord, Sydney, NSW, Australia*

BACKGROUND. Vitamin D is considered as an important determinant of bone turnover as well as cancer growth. Using a murine model of bone metastasis, we investigated the effect of vitamin D deficiency on prostate cancer cell growth in bone.
METHODS. Three-week-old male nude mice were fed either normal chow (control) or a diet deficient in vitamin D. The latter diet resulted in severe hypovitaminosis D within 6 weeks. At this point of time, 5×10^4 cells of the prostate cancer cell line, PC-3, were injected either into the bone marrow (tibia) or subcutaneously into soft tissues. Osteoprotegerin (OPG) was co-administered in subgroups of mice to suppress bone remodeling. Osteolytic lesions were monitored by serial X-ray, while soft tissue tumor growth was measured by caliper. All tissues were analyzed by micro-CT and histology at endpoint.
RESULTS. Bone turnover was significantly accelerated in vitamin D deficient compared to vitamin D sufficient mice from week 6 onwards. Intra-tibially implanted PC-3 cells resulted in mixed osteolytic and osteosclerotic lesion. At endpoint, osteolytic and osteosclerotic lesion areas, total tumor area, and tumor mitotic activity were all significantly increased in vitamin D deficient mice compared to controls. Regardless of diet, OPG reduced bone turnover, total tumor, and osteosclerotic area as well as tumor mitotic activity, while promoting cell apoptosis. In contrast, vitamin D deficiency did not alter tumor growth in soft tissues.
CONCLUSION. Vitamin D deficiency stimulates prostate cancer growth in bone through modulating the bone microenvironment. *Prostate 71: 1012–1021, 2011.*

KEY WORDS: **prostate cancer; bone metastasis; cancer growth; vitamin D deficiency; osteoclasts**

INTRODUCTION

Prostate cancer is the most common malignancy in men. The tumor has a high propensity to metastasize to the skeleton where the bone microenvironment plays an important role in supporting metastatic growth [1]. Bone remodeling seems to be an essential factor in this process, as inhibiting bone turnover alters metastasis rate and slows metastatic cancer growth in bone [2–5], while conversely, increased bone remodeling enhances skeletal cancer growth [6–10].

Vitamin D deficiency is common in the general population and its prevalence increases with age. Hypovitaminosis D leads to secondary hyperparathyroidism and high bone turnover. Importantly, the incidence of prostate cancer also rises with advancing age, thus coinciding with the peak in vitamin D

*Correspondence to: Markus J. Seibel, MD, PhD, FRACP, Bone Research Program, ANZAC Research Institute, University of Sydney, Concord, Sydney, NSW 2139, Australia.
E-mail: markus.seibel@sydney.edu.au
Received 18 July 2010; Accepted 8 November 2010
DOI 10.1002/pros.21316
Published online 28 December 2010 in Wiley Online Library (wileyonlinelibrary.com).

deficiency and bone remodeling rates. There is good epidemiological evidence that vitamin D deficiency is associated with prostate cancer incidence and related deaths [11,12], although the magnitude of this association seems inconsistent across clinical studies [13].

Peleg et al. [14] reported that daily injections of a low-calcemic vitamin D analog reduced osteoblastic lesions in a mouse model of prostate cancer metastasis in bone. In addition, calcitriol ($1,25(OH)_2D_3$) has been reported to have anti-proliferative, pro-differentiation, and pro-apoptotic actions on both normal and malignant cells derived from tissues such as skin, breast, prostate, or colon [15–19], suggesting that the bioactive vitamin D hormone may have direct inhibitory effects on cancer cell proliferation.

We previously reported that dietary calcium deficiency leads to increased bone remodeling and enhanced breast cancer growth in bone [9,10]. We reasoned that through a similar mechanism, vitamin D deficiency may also promote cancer growth in bone, either by increasing the osteoclast-mediated release of growth factors from the bone matrix, and/or through its direct effects on cancer cell proliferation. Recent observations from our group indicate that vitamin D deficiency enhances breast cancer growth in an *osteolytic* model of breast cancer bone metastasis [20], suggesting a causal link between vitamin D status and breast cancer growth in bone. As there is little direct experimental evidence of such relationships in prostate cancer, the present study aimed to define the effects of vitamin D deficiency on prostate cancer growth in a murine model of cancer metastasis to bone. Specifically, we hypothesized that vitamin D deficiency would promote prostate cancer tumor growth in bone via effects on bone remodeling that enhance tumor cell proliferation or survival. In addition, we investigated the direct effects of vitamin D on cancer cell growth in bone by inhibiting bone resorption and osteoclastogenesis by treatment with osteoprotegerin (OPG).

MATERIALS AND METHODS

Prostate Cancer Cell Line

The human prostate cancer cell line PC-3 was obtained from the American Type Culture Collection (ATCC, Manassas, VA). The cell line was cultured in Roswell Park Memorial Institute medium (RPMI) supplemented with 10% fetal calf serum (FCS, JRH Biosciences, KS) and 1% penicillin–streptomycin solution.

Cell Proliferation Assay and Gene Expression Studies

$1,25(OH)_2D_3$ (Sigma-Aldrich, St. Louis, MO) at concentrations of 10^{-7}, 10^{-8}, and 10^{-9} M or vehicle in RPMI supplemented with 2% FCS was added on day 1 to PC-3 cell cultures with replacement every 24 hr. Cells were counted daily for 6 days with Trypan blue (JRH Biosciences, KS) exclusion used to confirm cell viability. All experiments were repeated three times.

Additionally PC-3 cells were also seeded in 6-well plates at a density of 2×10^5 cells/well and subjected to total RNA extraction after treatment with 10^{-8} M $1,25(OH)_2D_3$ for 4 hr. Reverse transcription was performed to obtain cDNA for real-time RT-PCR assessment of VDR (GenBank accession no. NM_001017535), vitamin D 24-hydroxylase (CYP24, GenBank accession no. NM_000782), and vitamin D 1α-hydroxylase (CYP27B1α, GenBank accession no. NM_000785), using human-specific primers with iQ SYBR Green Supermix (Bio-Rad Laboratories, Hercules, CA) on an iCycler iQ5 real-time PCR detection system (Bio-Rad Laboratories). Human glyceraldehyde-3-phosphate dehydrogenase (GAPDH) gene expression was used for cDNA normalization.

Animals and Animal Maintenance

Male BALB/c nu/nu mice were obtained from the Animal Resources Centre, Canning Vale, WA, Australia. Mice were maintained under specific pathogen-free, temperature-controlled conditions throughout this study at the animal facilities of the ANZAC Research Institute in accordance with Institutional Animal Welfare Guidelines and an approved protocol. All mouse manipulations were performed inside a laminar-flow hood under aseptic conditions whilst maintaining general anesthesia with intra-peritoneal injection of ketamine/xylazine (75/10 mg/kg), unless otherwise noted.

Generation of Vitamin D Deficient Mice and Experimental Design

Our laboratory has established a protocol to induce and maintain long-term vitamin D deficiency in female nude mice, as described earlier [20]. Thirty-six 3-week-old male BALB/c nu/nu mice were given ad libitum either (i) normal mouse chow (vitamin D sufficient diet) containing 0.79% calcium and 2,000 IU/kg cholecalciferol (vitamin D_3) ($n = 18$), or (ii) a vitamin D free diet, identical in composition to (i) except for absence of cholecalciferol (Specialty Feeds, WA, Australia) ($n = 18$). Mice were housed in incandescent light conditions to minimize endogenous production of vitamin D.

At 8.5 weeks of age, mice on either diet were treated with either vehicle (0.9% sterile saline) or OPG at a dose of 3 mg/kg/3 days s.c., using a recombinant construct of OPG containing amino acids 22–194 of human OPG fused to the Fc domain of human immunoglobin G

(kindly provided by Amgen, Inc., Thousand Oaks, CA). This dose of OPG has been found previously to profoundly inhibit bone resorption in mice bearing osteolytic tumors [3]. As a result, there were four groups of n = 9 each for further experimentation: (1) vitamin D sufficient + saline; (2) vitamin D deficient + saline; (3) vitamin D sufficient + OPG; and (4) vitamin D deficient + OPG.

Three days after the introduction of saline or OPG, that is, at 9 weeks of age, all mice received an intra-tibial implantation of PC-3 cells, followed by X-ray monitoring for the development of osteolytic lesions at 2, 3, 4, and 5 weeks post-inoculation. Blood samples for measurement of plasma 25-hydroxy vitamin D (25D), tartrate-resistant acid phosphatase 5b (TRAcP5b), and mouse procollagen type I N-terminal propeptide (PINP) were obtained at the time of cell implantation (retro-orbital) and at sacrifice (cardiac puncture).

Intra-tibial Implantation

Log-phase growing cells were harvested by 0.02% EDTA and were then washed three times by centrifugation in phosphate-buffered saline (PBS) and subsequently resuspended in PBS (5×10^6 cells/ml). Cell viability >97% was determined by Trypan blue exclusion. Mice (n = 9/group) were anesthetized as described above and injected intra-tibially with 5×10^4 PC-3 cells suspended in 10 µl of PBS. The contralateral tibia was similarly injected with PBS and served as a control. Carprofen 5 mg/kg was administered s.c. at the time of inoculation to minimize post-surgical pain [3].

In Vivo Evaluation of Osteolytic Bone Lesions With X-Ray

For the in vivo assessment of osteolytic bone lesions, mice were anesthetized and assessed by digital radiography on days 21, 28, and 35. Experiments were terminated 5 weeks after cell implantation at which time mice in the non-OPG groups showed radiographic lesions $\geq 2\,mm^2$. Mice were anesthetized and examined again radiologically for osteolytic bone lesions before sacrifice and tissue harvest. Lytic bone areas were measured in injected and sham-injected tibiae on digitally recorded radiographs using an interactive image analysis software (ImageJ, NIH, USA).

Micro-CT Analysis

Micro-CT images were obtained using a SkyScan 1172 scanner (SkyScan, Kontich, Belgium) at 100 kV, 100 AA with a 1 mm aluminum filter. For each specimen, 1,800 cross-sectional projections were collated at a resolution of 6.93 Am/pixel. Sections were reconstructed using a modified Feldkamp cone-beam algorithm, with beam hardening correction set to 50%. Three-dimensional (3D) modeling from the reconstructed sections was achieved using the VGStudio MAX v1.2 software (Volume Graphics GmbH, Heidelberg, Germany). The reconstructed 3D model of tibiae was then used to create two-dimensional (2D) images showing three different view-planes around the tibiae. These included the three general faces of the diaphysis (i.e., anterior, lateral, and posterior views). This process was replicated for all the scans to produce the samples used for the analysis. The osteolytic area in each image, representing areas of complete perforation of the cortex, was measured using ImageJ software. Total lytic area was the sum of measurements from the three images for each sample. Osteosclerotic changes were quantified on the same micro-CT images as that for osteolysis.

Biochemical Assays

Plasma levels of 25(OH)D, tartrate-resistant acid phosphatase band 5b (TRAcP5b, a bone resorption marker) and mouse procollagen type I aminoterminal propeptide (PINP, a bone formation marker) were measured by specific immunoassay (Immunodiagnostic Systems Ltd, Boldon, UK). The assay for 25(OH)D has a sensitivity of 5 nmol/L and an intra-assay coefficient of variation (CV) of 5.6%. The assay for TRAcP5b has a sensitivity of 0.1 U/L and an intra-assay CV of 6.5%, while the PINP assay has a sensitivity of 0.7 ng/ml, an intra-assay CV of 7.4%.

Histological Assessment

Tibiae were fixed for 36 hr in 4% paraformaldehyde buffered with 0.1 M phosphate buffer (pH 7.4) and decalcified in 10% EDTA at 4°C for 2 weeks. The tissues were then processed and embedded in paraffin. Five-micron sections were cut from each specimen and stained with hematoxylin and eosin for routine histological examination. Histochemical examination for tartrate-resistant acid phosphatase (TRAcP), as a marker for osteoclasts, was performed by using naphthol AS-BI phosphate (Sigma Chemical Co., St. Louis, MO) as a substrate and fast red violet Luria-Bertani salt (Sigma) as a stain for the reaction product; incubation was performed at room temperature for 30 min [3]. Tumor sections were analyzed for mitotic activity [21] and stained with by terminal deoxynucleotidyl transferase-mediated dUTP nick end labeling (TUNEL), which was done on 5-µm sections with the In situ Cell Death Detection kit, POD (Roche Diagnostics), according to the manufacturer's protocol. The ratio of mitotic cells and apoptotic TUNEL stained cells was

determined by counting positive and negative cells in five random fields of non-necrotic areas of tumors in a representative section in each bone specimen (400× magnification).

Bone Histomorphometry

Histomorphometric analysis of the proximal tibial metaphysis was conducted to evaluate bone volume and tumor burden. Measurements were performed in longitudinal 5 μm sections stained with hematoxylin and eosin or reacted to show TRAcP activity (12.5× magnification) with measurement made interactively using the OsteoMeasure System (Osteometrics, Atlanta, GA). To determine tumor area, three sagittal sections through the tibia were taken at approximately 200 μm intervals, representing upper, mid, and lower regions of the proximal tibia. Total tumor area was measured in each section and the average tumor area was used as an index of tumor burden. Cortical bone area was measured in the same sections. New woven bone formation was measured as osteosclerotic bone area in the same sections as previously described [10]. Osteoclasts were identified as TRAcP positive multinucleated cells associated with bone surfaces. The osteoclast number (200× magnifications) per millimeter square of osteosclerotic lesion area was calculated.

Subcutaneous Implantation of PC-3 Cells

Cells were prepared as above and suspended in cold 50% Matrigel: PBS at a concentration of 2×10^7 cells/ml. One hundred microliters of the suspension was implanted subcutaneously into the flank of mice ($n = 5$). Tumor size was measured serially by caliper to determine tumor volume [22].

Statistical Analysis

All data were presented as the mean ± SE unless indicated otherwise. Statistics were done using Student's *t*-test by means of SPSS 17.0 for Windows (SPSS, Inc., Chicago, IL) for simple comparison of two means. For multiple comparisons, analyses utilized one-way ANOVA followed post hoc by *Tukey's* test. Significance was accepted where $P < 0.05$.

RESULTS

Calcitriol Directly Inhibits Prostate Cancer Cell Proliferation In Vitro

The PC-3 cell line expressed the VDR and responded to treatment with calcitriol (1,25-dihydroxy vitamin D; $1,25(OH)_2D_3$). When treated with 10^{-8} M of 1,25 $(OH)_2D_3$ for 4 hr, expression of CYP24 and the VDR increased by eight- and twofold, respectively, consistent with the activation of the VDR and of the VDR-responsive gene encoding for the $1,25(OH)_2D_3$ inactivating enzyme, 24-hydroxylase (Fig. 1A). Conversely, $1,25(OH)_2D_3$ down-regulated the $25(OH)D_3$-activating enzyme, 1α-hydroxylase (CYP27B1α) by approximately 50% (Fig. 1A). The maximal inhibitory effects of $1,25(OH)_2D_3$ on cell proliferation were found at a dose of approximately 10^{-8} M, which after 6 days in culture resulted in a 30% reduction in cell numbers (Fig. 1B).

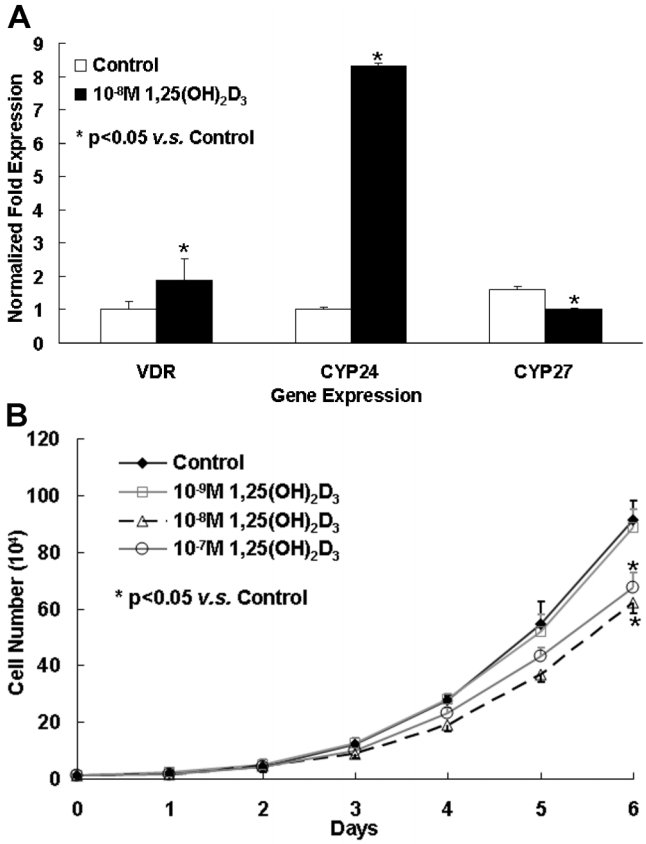

Fig. 1. PC-3 prostate cancer cells respond to 10^{-8} M calcitriol ($1,25(OH)_2D_3$) after 4 hr treatment. **A**: PC-3 cells express VDR and are stimulated by $1,25(OH)_2D_3$ to up-regulate VDR expression by approximately twofold. The $1,25(OH)_2D_3$ inactivating enzyme, 24-hydroxylase (CYP24) is strongly induced (eightfold) by $1,25(OH)_2D_3$. The 25(OH)D activating enzyme, 1α-hydroxylase (CYP27B1) is marginally down-regulated by about 0.5-fold when cells are treated with $1,25(OH)_2D_3$. All gene expression results are representative of three independent experiments. *$P < 0.01$, compared to controls. **B**: Growth of PC-3 cells is inhibited by $1,25(OH)_2D_3$. Growth curves for PC-3 cells when treated with varying concentrations of $1,25(OH)_2D_3$. The maximal inhibitory concentration was 10^{-8} M $1,25(OH)_2D_3$. Results are representative of three independent experiments. *$P < 0.05$ compared to controls (group $n = 3$).

Dietary Vitamin D Restriction Induces Vitamin D Deficiency

Blood samples taken at the time of cancer cell implantation and at sacrifice 5 weeks later confirmed pronounced vitamin D deficiency in male nude mice fed a vitamin D deficient diet, with a mean ± SD plasma 25(OH)D level of 6.9 ± 1.8 nmol/L (n = 9). In contrast, mice on regular diet were vitamin D replete with a mean ± SD plasma 25(OH)D level of 97.9 ± 10.1 nmol/L (n = 9). Plasma TRAcP5b and PINP levels were significantly increased in vitamin D deficient compared to vitamin D sufficient mice at week 6 (Fig. 2A), signifying accelerated bone turnover.

At week 11, vitamin D deficient mice maintained significantly lower plasma 25(OH)D levels compared to their vitamin D replete counterparts (5.3 ± 1.8 nmol/L vs. 107.4 ± 10.3 nmol/L) (n = 9). Plasma PINP levels were also significantly higher in vitamin D deficient than D sufficient mice, however, TRAcP5b levels were similar in both groups by that time (n = 9). In the OPG treated groups, vitamin D status was similar to that in groups on either diet alone. In contrast, plasma PINP and TRAcP5b levels were profoundly reduced by OPG treatment (n = 9) (Fig. 2B,C). At all time points, vitamin D deficient mice had similar body weights as mice on a normal diet (data not shown).

Vitamin D Deficiency Promotes Prostate Cancer Growth in the Tibial Metaphysis

Following the injection of PC-3 cells into bone, the development of osteolytic lesions was monitored by X-ray and, at endpoint, analyzed by micro-CT imaging. Radiographic lytic lesions appeared earlier and progressed faster in vitamin D deficient than in vitamin D replete mice. At endpoint, osteolytic lesions were significantly larger in vitamin D deficient than in vitamin D sufficient mice, as assessed by both X-ray (+68%) and micro-CT analysis (+296%; $P < 0.05$ for both) (n = 9). Treatment with OPG completely inhibited the development of lytic lesions (Fig. 3A,B).

Although there was a predominance of lytic activity seen on X-ray and micro-CT imaging, smaller sclerotic changes were clearly visible in the vitamin D deficient mice (Fig. 3A, arrows). By day 35, vitamin D deficient mice developed significantly larger osteosclerotic lesions then vitamin D replete animals as quantified by micro-CT imaging (Fig. 3C). Osteosclerotic changes were not measured in OPG treated mice as it was difficult to differentiate between tumor-induced and OPG-induced osteosclerosis.

Histological assessment of tumor-bearing tibiae revealed the presence of new woven bone in close proximity to the tumor, consistent with tumor-induced osteosclerosis. While histological analysis of total tumor area confirmed that metastatic depots were larger in vitamin D deficient than vitamin D replete mice (tumor: +50%; Fig. 4A) (n = 9), it also revealed that the extent of osteosclerosis was increased by 50% in vitamin D deficient compared to vitamin D sufficient mice (Fig. 4B). Cortical bone areas were significantly reduced in vitamin D deficient mice compared with those in vitamin D sufficient mice (−29%, Fig. 4C), consistent with the greater lytic lesions found on radiographic imaging. Anti-resorptive treatment with OPG reduced both total tumor area (−44% and −40%,

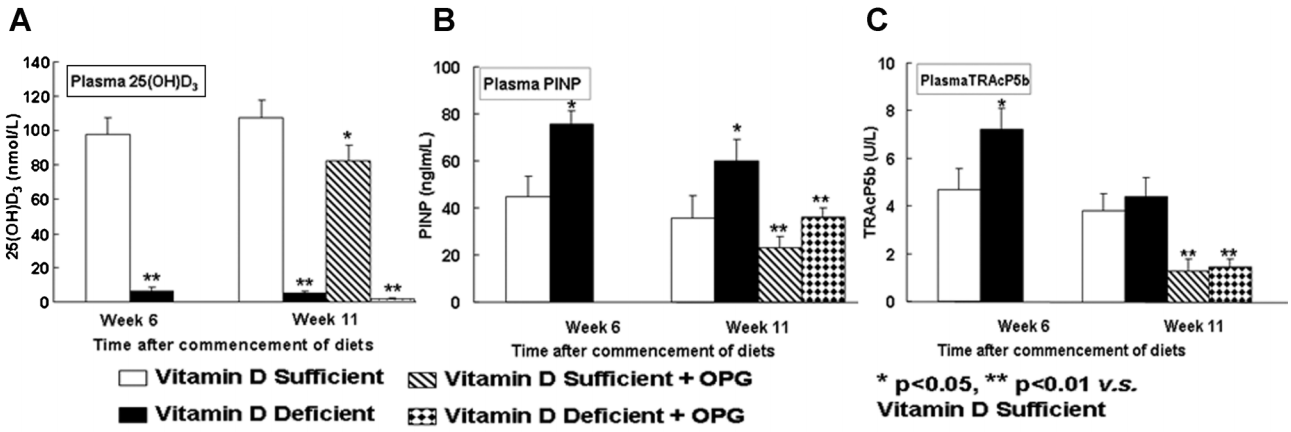

Fig. 2. Biochemical assessment of mice receiving vitamin D deficient or vitamin D sufficient diets. **A**: Plasma 25(OH)D levels are profoundly reduced at 6 and 11 weeks, independent of concomitant OPG treatment. **B**,**C**: Plasma levels of PINP and TRAcP5b were significantly increased in vitamin D deficient mice at week 6. At week 11, plasma PINP levels were still significantly higher in vitamin D deficient compared to vitamin D sufficient mice. There was no difference between TRAcP5b levels. In OPG-treated mice, bone turnover as determined by plasma TRAcP5b and PINP was profoundly suppressed, while vitamin D status remained unaffected. Data are shown as mean ± SD for group sizes of n = 9. *$P < 0.05$, **$P < 0.01$, compared to vitamin D sufficient mice.

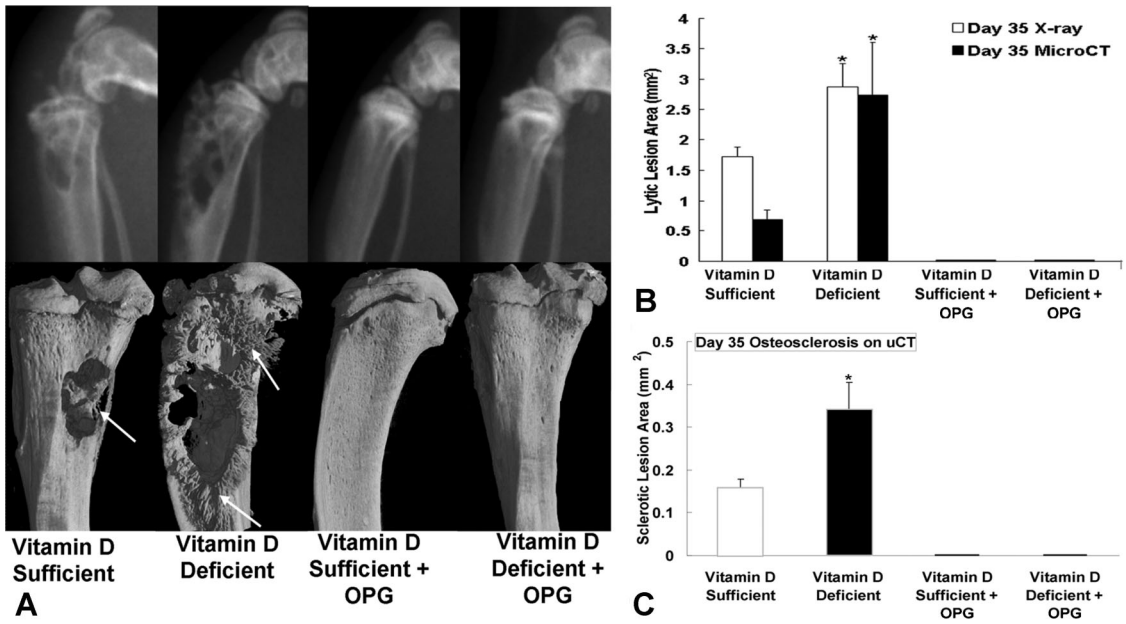

Fig. 3. Osteolytic lesions as monitored by X-ray and micro-CT imaging. **A**–**C**: By day 35, vitamin D deficient mice had developed significantly larger osteolytic (B) and osteosclerotic lesions (C) than vitamin D sufficient mice (arrows indicate sclerotic lesions). In contrast, OPG treatment completely inhibited the development of osteolytic lesions. Osteosclerotic changes were not measured in OPG treated mice as it was difficult to differentiate between tumor-induced and OPG-induced effects. Data are shown as mean ± SE for group sizes of n = 9. *$P < 0.05$, compared to vitamin D sufficient mice.

respectively) and osteosclerotic lesion area (−48% and −38%, respectively), and protected cortical bone in both groups of animals (n = 9) (Fig. 4A–C).

Tumors from vitamin D deficient mice had higher mitotic activity compared to vitamin D sufficient mice (+56%), whereas both groups showed similar numbers of TUNEL-positive apoptotic cells. In contrast, OPG treatment significantly reduced the proportion of actively dividing cells in both diet groups (−32% and −33%, respectively) and increased rates of cell apoptosis (+124% and +113%, respectively, n = 9) (Fig. 4D,E).

Osteoclast numbers at the tumor bone interface in vitamin D deficient mice were not significantly different from vitamin D sufficient mice groups (16.2 ± 2.9/mm vs. 14.7 ± 3.14/mm, respectively), although there was a trend for more osteoclasts in vitamin D deficient mice. Osteoclast differentiation and activity were inhibited by OPG treatment, as no TRAcP positive osteoclasts were detected in sections from OPG treated mice.

Vitamin D Deficiency Does Not Alter Tumor Growth in Soft Tissues

Growth rates of tumors implanted subcutaneously into the soft tissue (measured as a progressive increase in tumor volume) were similar at all time points (Fig. 5A). Final tumor weights were similar in both vitamin D sufficient and deficient mice (0.39 ± 0.10 g vs. 0.40 ± 0.17 g) (n = 5) (Fig. 5B).

DISCUSSION

The current study demonstrates that vitamin D deficiency strongly promotes the growth of prostate cancer cells in bone but not in soft tissues. Concurrent anti-resorptive treatment with OPG significantly reduced tumor growth in bone, indicating that secondary changes in the bone microenvironment play a critical role in mediating the effect of vitamin D on cancer cell behavior.

Severe hypovitaminosis D usually leads to secondary hyperparathyroidism and, as a consequence to accelerated bone turnover. There is good epidemiological evidence of an inverse relationship between vitamin D status and prostate cancer progression, such that men with low vitamin D status appear to have worse outcomes from prostate cancer [23]. Although there have been no longitudinal clinical studies in men addressing this question, a clinical study in women demonstrated that vitamin D deficiency was associated with increased breast cancer incidence and poorer overall prognosis [24]. Furthermore, recent clinical studies suggest that increased levels of bone turnover at the time of diagnosis or during or after chemotherapy are associated with a higher risk of skeletal-related events and poor survival in patients with malignancies

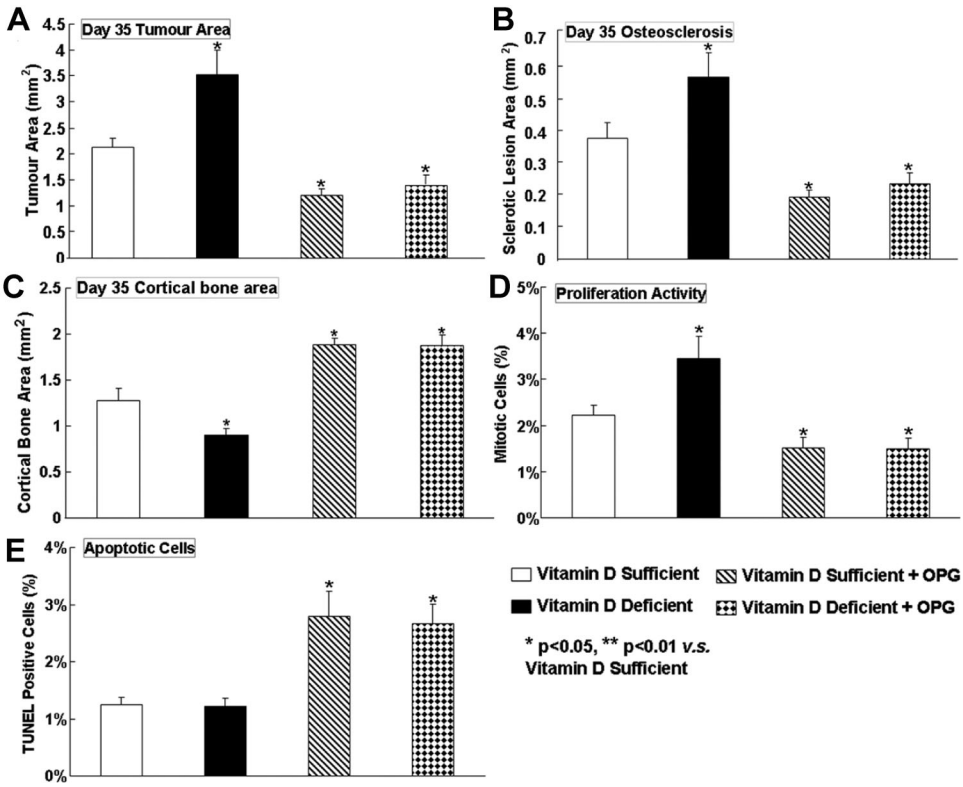

Fig. 4. Effect of vitamin D deficiency on tumor growth in bone with or without concurrent OPG treatment. **A**,**B**: Vitamin D deficient mice developed larger tumor and osteosclerotic lesions areas than vitamin D sufficient mice. OPG treatment drastically suppressed tumor expansion and osteosclerotic lesion areas in both vitamin D sufficient and vitamin D deficient mice. **C**: Cortical bone areas were significantly reduced in vitamin D deficient compared with to vitamin D sufficient mice. Treatment with OPG completely protected cortical bone from lytic activity. **D**,**E**: Tumors from vitamin D deficient mice demonstrated higher mitotic activity than those taken from vitamin D sufficient mice. TUNEL-positive, apoptotic cell numbers were similar in both groups. OPG reduced the number of mitotic events and increased the number of TUNEL-positive cells in both groups. Data are shown as mean ± SE for group sizes of n = 9, $^*P < 0.05$.

as diverse as prostate, breast, lung and renal cancer, or multiple myeloma [25–28].

Several animal studies convincingly demonstrated that high bone resorption promotes tumor progression in bone [6–8]. We have previously demonstrated that both calcium deficiency [9,10] and vitamin D deficiency [20] in isolation enhances tumor growth in a model of *breast* cancer bone metastasis. However, as there is little

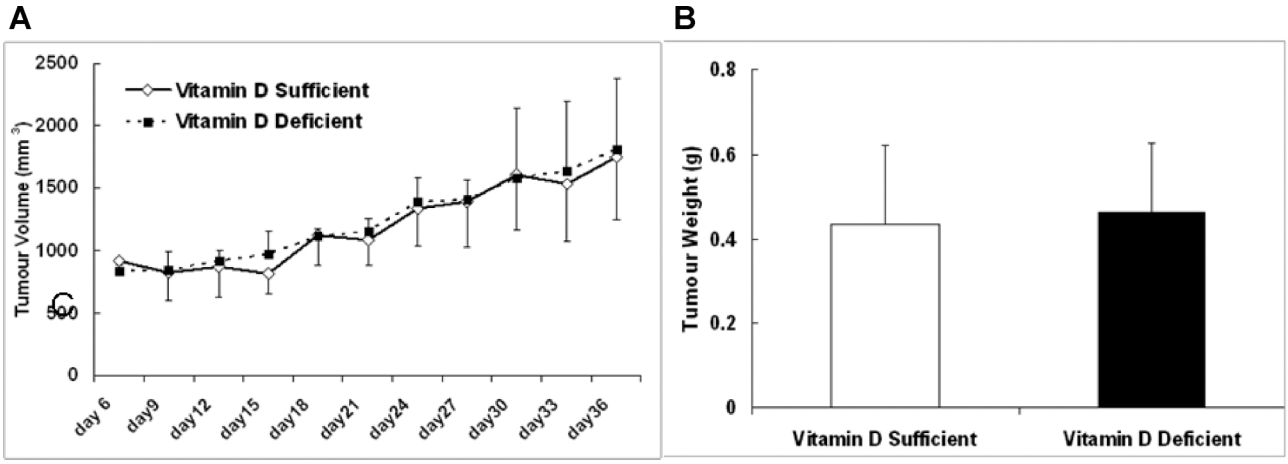

Fig. 5. Vitamin D deficiency does not alter subcutaneous tumor growth. Tumor growth rates (**A**) and final tumor weights (**B**) for subcutaneous tumors were similar at all time points in vitamin D sufficient and deficient mice. Data are shown as mean ± SD for group sizes of n = 5, $P > 0.05$.

experimental evidence of similar effects in prostate cancer, and to substantiate our previous findings in a biologically diverse tumor type, the present study aimed to establish whether there is a causal relationship between vitamin D deficiency, bone turnover and prostate cancer progression in bone. To this aim, we successfully induced vitamin D deficiency in male nude mice, which resulted in significantly accelerated bone turnover (the gradual decline in absolute TRAcP5b and PINP levels in both groups of mice is expected, due to slowing growth rates associated with normal aging).

In men, prostate cancer bone metastases are frequently osteosclerotic. However, histological evidence indicates that these metastases are always composed of a heterogeneous mixture of osteolytic and osteosclerotic lesions [2,29], with a net excess of bone formation over bone resorption. In our studies, PC-3 cells formed predominantly osteolytic lesions in the bones of nude mice, with a smaller osteosclerotic component. While osteoclastic activity predominates in osteolytic tumors, it has been suggested that in osteosclerotic bone metastasis both osteoclasts and osteoblasts are active and could each act to support tumor growth. In this study with prostate cancer cells, and in previous studies with C4-2B prostate cancer cells and MCF-7 cells [2,30], anti-resorptive treatment with OPG inhibited tumor growth and the size of osteosclerotic lesions. OPG treatment directly inhibits osteoclastogenesis and thus bone resorption, but via coupling, also indirectly inhibits bone formation [2,3]. It is likely that in the current study changes in bone resorption mediate the enhanced tumor growth induced by vitamin D deficiency, and the reversal of this effect with OPG treatment. However, a contribution of altered osteoblastic activity to the changes in prostate cancer growth cannot be ruled out. Both bone resorption and bone formation effects may be important in prostate cancer when the tumor causes both osteolytic and osteosclerotic changes.

In the current study, we also used reconstructed 3D micro-CT image analysis for the calculation of osteolytic areas and compared the results with those obtained from 2D X-ray imaging. Micro-CT measurements generally paralleled X-ray measurements although osteolytic areas were somewhat smaller as a result of the micro-CT detecting complete cortical perforations whereas X-ray analysis also detects cortical thinning and trabecular bone loss (Fig. 3B). The micro-CT images also revealed areas of periosteal osteosclerosis.

Faster skeletal tumor growth in vitamin D deficient mice may be due to several factors. Vitamin D deficiency induces hyperparathyroidism [23,31] and leads to an increase in bone resorption. These changes are similar to those reported in humans diagnosed with pronounced hypovitaminosis D [32]. Consistent with the findings from our and other groups, enhanced cancer cell growth in bone has been reported in association with treatments that increase bone resorption rates [6–10,20]. With vitamin D deficiency augmenting bone turnover, it is likely that increased bone resorption promotes tumor growth via the vicious cycle proposed by Mundy [1]. Bone resorption activity (assessed by serum TRAcP5b) was significantly elevated at the time of tumor implantation in the vitamin D deficiency group, but at the endpoint in our study, there were no differences between the two groups in either osteoclast number or bone resorption activity (as assessed by serum TRAcP5b). This discrepancy could be due to the adaptation of mice to a vitamin D deficient diet or, alternatively, to pro-resorptive local tumor effects dominating the effects of elevated systemic PTH levels [9,20].

In addition to its effects on the bone microenvironment, there may be direct effects of vitamin D on tumor growth. Vitamin D deficiency may remove vitamin D dependent inhibition of tumor cell proliferation. Thus, next to its known role in calcium and phosphate metabolism, the metabolically active form of vitamin D, 1,25-dihydroxyvitamin D ($1,25(OH)_2D$) appears to have further autocrine and paracrine functions. We demonstrated that the PC-3 cells express the VDR, and that $1,25(OH)_2D_3$ up-regulated VDR and CYP24 expression. This cell line also expresses CYP27B1α (encoding 1α-hydroxylase) and thus may be able to locally convert 25(OH)D to metabolically active $1,25(OH)_2D$. In the presence of exogenous $1,25(OH)_2D_3$, a modest down-regulation of CYP27B1α was noted in our experiments, suggesting the operation of a negative feedback loop on endogenous $1,25(OH)_2D$ synthesis.

Our results indicate that $1,25(OH)_2D_3$ has direct antiproliferative effects on PC-3 cells, consistent with observations of others showing a dose-dependent inhibition of cancer cell proliferation in vitro (breast, colon, thyroid, skin, head, and neck) by $1,25(OH)_2D_3$ [15–19]. Alternative mechanisms for the effects of vitamin D deficiency in vivo could include immune modulation [33] or loss of the direct effects of $25(OH)D_3$ on tumor cells. The lack of significant effects of vitamin D deficiency on the growth of PC-3 cells implanted subcutaneously and the loss of effects at later time points in the tibia suggest that the effects of vitamin D deficiency on tumor growth may be site or stage specific.

In summary, the current experimental in vivo study demonstrates that vitamin D deficiency promotes prostate cancer growth in bone. Concurrent suppression of bone turnover with OPG treatment significantly

reduced the growth of prostate cancer in bone, regardless of vitamin D status, indicating an important role for the bone microenvironment. Our results suggest that maintenance of adequate vitamin D levels is potentially of clinical importance, particularly in populations with, or at high risk of prostate cancer. Clinical trials are indicated to investigate the value of correcting vitamin D deficiency in limiting the progression of prostate cancer and its metastatic process.

ACKNOWLEDGMENTS

We thank the Prostate Cancer Foundation of Australia (PCFA) for their generous financial support through a 2-year concept grant. We thank Mamdouh Khalil and his staff for the excellent animal care. We thank Dr Yu-Tat POON and the staff from Radiology Department of Concord Hospital, Sydney, for their great assistance in X-ray analysis. The authors also acknowledge the technical assistance from the staff at the NANO Major National Research Facility at the Electron Microscope Unit, University of Sydney. We thank Amgen, Inc., Thousand Oaks, for the provision of osteoprotegerin.

REFERENCES

1. Mundy GR. Metastasis to bone: Causes, consequences and therapeutic opportunities. Nat Rev Cancer 2002;2(8):584–593.
2. Zhang J, Dai J, Qi Y, Lin DL, Smith P, Strayhorn C, Mizokami A, Fu Z, Westman J, Keller ET. Osteoprotegerin inhibits prostate cancer-induced osteoclastogenesis and prevents prostate tumor growth in the bone. J Clin Invest 2001;107(10):1235–1244.
3. Zheng Y, Zhou H, Brennan K, Blair JM, Modzelewski JR, Seibel MJ, Dunstan CR. Inhibition of bone resorption, rather than direct cytotoxicity, mediates the anti-tumour actions of ibandronate and osteoprotegerin in a murine model of breast cancer bone metastasis. Bone 2007;40(2):471–478.
4. Morony S, Capparelli C, Sarosi I, Lacey DL, Dunstan CR, Kostenuik PJ. Osteoprotegerin inhibits osteolysis and decreases skeletal tumor burden in syngeneic and nude mouse models of experimental bone metastasis. Cancer Res 2001;61(11):4432–4436.
5. Neudert M, Fischer C, Krempien B, Bauss F, Seibel MJ. Site-specific human breast cancer (MDA-MB-231) metastases in nude rats: Model characterisation and in vivo effects of ibandronate on tumour growth. Int J Cancer 2003;107(3):468–477.
6. Schneider A, Kalikin LM, Mattos AC, Keller ET, Allen MJ, Pienta KJ, McCauley LK. Bone turnover mediates preferential localization of prostate cancer in the skeleton. Endocrinology 2005; 146(4):1727–1736.
7. Price JT, Quinn JM, Sims NA, Vieusseux J, Waldeck K, Docherty SE, Myers D, Nakamura A, Waltham MC, Gillespie MT, Thompson EW. The heat shock protein 90 inhibitor, 17-allylamino-17-demethoxygeldanamycin, enhances osteoclast formation and potentiates bone metastasis of a human breast cancer cell line. Cancer Res 2005;65(11):4929–4938.
8. Hirbe AC, Uluckan O, Morgan EA, Eagleton MC, Prior JL, Piwnica-Worms D, Trinkaus K, Apicelli A, Weilbaecher K. Granulocyte colony-stimulating factor enhances bone tumor growth in mice in an osteoclast-dependent manner. Blood 2007;109(8):3424–3431.
9. Zheng Y, Zhou H, Modzelewski JR, Kalak R, Blair JM, Seibel MJ, Dunstan CR. Accelerated bone resorption, due to dietary calcium deficiency, promotes breast cancer tumor growth in bone. Cancer Res 2007;67(19):9542–9548.
10. Zheng Y, Zhou H, Fong-Yee C, Modzelewski JR, Seibel MJ, Dunstan CR. Bone resorption increases tumour growth in a mouse model of osteosclerotic breast cancer metastasis. Clin Exp Metastasis 2008;25(5):559–567.
11. Lagunova Z, Porojnicu AC, Dahlback A, Berg JP, Beer TM, Moan J. Prostate cancer survival is dependent on season of diagnosis. Prostate 2007;67(12):1362–1370.
12. Tuohimaa P, Tenkanen L, Ahonen M, Lumme S, Jellum E, Hallmans G, Stattin P, Harvei S, Hakulinen T, Luostarinen T, Dillner J, Lehtinen M, Hakama M. Both high and low levels of blood vitamin D are associated with a higher prostate cancer risk: A longitudinal, nested case–control study in the Nordic countries. Int J Cancer 2004;108(1):104–108.
13. Ahn J, Peters U, Albanes D, Purdue MP, Abnet CC, Chatterjee N, Horst RL, Hollis BW, Huang WY, Shikany JM, Hayes RB. Serum vitamin D concentration and prostate cancer risk: A nested case–control study. J Natl Cancer Inst 2008;100(11):796–804.
14. Peleg S, Khan F, Navone NM, Cody DD, Johnson EM, Van Pelt CS, Posner GH. Inhibition of prostate cancer-meditated osteoblastic bone lesions by the low-calcemic analog 1alpha-hydroxymethyl-16-ene-26,27-bishomo-25-hydroxy vitamin D3. J Steroid Biochem Mol Biol 2005;97(1–2):203–211.
15. Peng X, Hawthorne M, Vaishnav A, St-Arnaud R, Mehta RG. 25-Hydroxyvitamin D3 is a natural chemopreventive agent against carcinogen induced precancerous lesions in mouse mammary gland organ culture. Breast Cancer Res Treat 2009;113(1):31–41.
16. Townsend K, Banwell CM, Guy M, Colston KW, Mansi JL, Stewart PM, Campbell MJ, Hewison M. Autocrine metabolism of vitamin D in normal and malignant breast tissue. Clin Cancer Res 2005;11(9):3579–3586.
17. Cross HS, Lipkin M, Kallay E. Nutrients regulate the colonic vitamin D system in mice: Relevance for human colon malignancy. J Nutr 2006;136(3):561–564.
18. Pendas-Franco N, Gonzalez-Sancho JM, Suarez Y, Aguilera O, Steinmeyer A, Gamallo C, Berciano MT, Lafarga M, Munoz A. Vitamin D regulates the phenotype of human breast cancer cells. Differentiation 2007;75(3):193–207.
19. Rohan JN, Weigel NL. 1Alpha,25-dihydroxyvitamin D3 reduces c-Myc expression, inhibiting proliferation and causing G1 accumulation in C4-2 prostate cancer cells. Endocrinology 2009;150(5):2046–2054.
20. Ooi LL, Zhou H, Kalak R, Zheng Y, Conigrave AD, Seibel MJ, Dunstan CR. Vitamin d deficiency promotes human breast cancer growth in a murine model of bone metastasis. Cancer Res 2010;70(5):1835–1844.
21. Bult P, Manders P, Straatman HM, Tjan-Heijnen VC, Beex LV, Hendriks J, Leer JW, Verbeek AL, Holland R. In primary breast cancer the mitotic activity yields similar prognostic information as the histological grade: A study with long-term follow-up. Breast Cancer Res Treat 2010;122(1):77–86.
22. Mehta RR, Graves JM, Hart GD, Shilkaitis A, Das Gupta TK. Growth and metastasis of human breast carcinomas with Matrigel in athymic mice. Breast Cancer Res Treat 1993;25(1): 65–71.
23. Garland CF, Garland FC, Gorham ED, Lipkin M, Newmark H, Mohr SB, Holick MF. The role of vitamin D in cancer prevention. Am J Public Health 2006;96(2):252–261.

24. Goodwin PJ, Ennis M, Pritchard KI, Koo J, Hood N. Prognostic effects of 25-hydroxyvitamin D levels in early breast cancer. J Clin Oncol 2009;27(23):3757–3763.
25. Woitge HW, Horn E, Keck AV, Auler B, Seibel MJ, Pecherstorfer M. Biochemical markers of bone formation in patients with plasma cell dyscrasias and benign osteoporosis. Clin Chem 2001;47(4):686–693.
26. Ali SM, Demers LM, Leitzel K, Harvey HA, Clemens D, Mallinak N, Engle L, Chinchilli V, Costa L, Brady C, Seaman J, Lipton A. Baseline serum NTx levels are prognostic in metastatic breast cancer patients with bone-only metastasis. Ann Oncol 2004; 15(3):455–459.
27. Brown JE, Cook RJ, Major P, Lipton A, Saad F, Smith M, Lee KA, Zheng M, Hei YJ, Coleman RE. Bone turnover markers as predictors of skeletal complications in prostate cancer, lung cancer, and other solid tumors. J Natl Cancer Inst 2005;97(1): 59–69.
28. Cook RJ, Coleman R, Brown J, Lipton A, Major P, Hei YJ, Saad F, Smith MR. Markers of bone metabolism and survival in men with hormone-refractory metastatic prostate cancer. Clin Cancer Res 2006;12 (11 Pt 1):3361–3367.
29. Dai J, Hall CL, Escara-Wilke J, Mizokami A, Keller JM, Keller ET. Prostate cancer induces bone metastasis through Wnt-induced bone morphogenetic protein-dependent and independent mechanisms. Cancer Res 2008;68(14):5785–5794.
30. Kiefer JA, Vessella RL, Quinn JE, Odman AM, Zhang J, Keller ET, Kostenuik PJ, Dunstan CR, Corey E. The effect of osteoprotegerin administration on the intra-tibial growth of the osteoblastic LuCaP 23.1 prostate cancer xenograft. Clin Exp Metastasis 2004;21(5):381–387.
31. Holick MF. Optimal vitamin D status for the prevention and treatment of osteoporosis. Drugs Aging 2007;24(12):1017–1029.
32. Vieth R, Chan PC, MacFarlane GD. Efficacy and safety of vitamin D3 intake exceeding the lowest observed adverse effect level. Am J Clin Nutr 2001;73(2):288–294.
33. Peterlik M, Cross HS. Vitamin D and calcium deficits predispose for multiple chronic diseases. Eur J Clin Invest 2005;35(5): 290–304.